Antiproton Stopping at Low Energies: Confirmation of Velocity-Proportional Stopping Power

S. P. Møller,[1] A. Csete,[2] T. Ichioka,[2] H. Knudsen,[2] U. I. Uggerhøj,[2] and H. H. Andersen[3]

[1]*Institute for Storage Ring Facilities, University of Aarhus, DK-8000 Aarhus C, Denmark*

[2]*Institute of Physics and Astronomy, University of Aarhus, DK-8000 Aarhus C, Denmark*

[3]*Ørsted Laboratory, Niels Bohr Institute, Universitetsparken 5, DK-2100 København Ø, Denmark*

(Received 3 December 2001; published 25 April 2002)

The stopping power for antiprotons in various solid targets has been measured in the low-energy range of 1–100 keV. In agreement with most models, in particular free-electron gas models, the stopping power is found to be proportional to the projectile velocity below the stopping-power maximum. Although a stopping power proportional to velocity has also been observed for protons, the interpretation of such measurements is difficult due to the presence of charge exchange processes. Hence, the present measurements constitute the first unambiguous support for a velocity-proportional stopping power due to target excitations by a pointlike projectile.

DOI: 10.1103/PhysRevLett.88.193201 PACS numbers: 29.30.Aj, 34.50.Bw

The penetration of charged particles through matter has been of interest since the discovery of atomic particles [1], and, in particular, the slowing-down process has been a test bed for the development of new theoretical approaches. The slowing down is mainly characterized by the stopping power $-dE/dx$, which at low velocities is widely accepted to be proportional to the projectile velocity. Indeed, several theoretical approaches to the stopping at low energy, in particular, the free electron-gas description [2], arrive at velocity proportional stopping power. For a metal, one would expect such a free-electron gas description to be good for the conduction electrons, but certainly not for tightly bound inner-shell electrons. Recently a "threshold effect" was indeed observed in the energy loss of protons due to inner-shell electrons [3]. However, it should be borne in mind that it is the loosely bound electrons that give the dominating contribution to the stopping power at low energy. In the considered low-energy region electronic stopping dominates, i.e., the main energy transfers are due to electronic excitations, and we may neglect the nuclear collisions where target atoms recoil as a whole.

On the experimental side, stopping powers have been studied from low to very high projectile energies using both light and heavy ions. The experimental investigations have at least partly been spurred by the need for accurate stopping powers for many practical applications, including ion implantation and radiation therapy. One of the benefits of studying stopping powers with negative particles is, in addition to their fundamental interest, that theoretical approaches become much simpler since electron capture is excluded. A velocity-linear stopping power, as predicted by, e.g., free-electron-gas models, is observed for positive particles, but the interpretation is hampered by a significant contribution from charge exchange processes. In fact, deviations from a velocity-linear stopping power for protons at low energies have been found only in the case of He [4] and Ne [5] targets, and even for large-band-gap insulators, a velocity proportional stopping power was surprisingly observed [6]. The observed stopping power could be reproduced only by calculations which included electron promotion processes, where electrons are promoted to molecularlike orbitals [6]. Hence the issues concerning velocity-proportional stopping power in the fundamental slowing-down process are most directly studied with pointlike projectiles of negative charge.

A difference between the stopping power for positive and negative pointlike particles, what is nowadays called the Barkas effect, was first observed for pions [7]. The reduction in stopping power for fast particles of a negative as compared to a positive charge is due to a polarization effect and has since its discovery been studied with a variety of particles. Accurate measurements have, however, been obtained only within the last decade with antiprotons (and protons) in the energy interval 50 keV–5 MeV; see [8] and references therein. In this energy range, at and above the stopping power maximum, the Barkas effect is a perturbation to the Bethe description of stopping. These two subjects — the velocity-proportional stopping power and the Barkas effect — form the motivation for the present study.

The continuation of our previous antiproton measurements at LEAR [8] was conducted at the antiproton decelerator (AD) at CERN [9]. The AD machine delivers around 10^7 antiprotons in a pulse of 0.5 μs duration at a kinetic energy of 5.3 MeV with a repetition time of about 2 min. A radio frequency quadrupole (RFQ) subsequently decelerates this beam [10]. The output energy of this decelerator can be varied, although the tuning is tedious, between 0 and 120 keV, and the efficiency approaches 40% at not too low energies. In passing, we note that this RFQ decelerator is the first successfully operating decelerating RFQ in the world, a major accomplishment in itself. The experimental apparatus (see Fig. 1), used in the determination of the stopping powers, has been described in detail in [11]. It differs from the usual equipment to measure stopping power, since it was designed to measure stopping powers with the rather special antiproton beam available at the AD. In short, it is based on two 90° electrostatic spherical analyzers (ESA). Since the energy spread of the beam

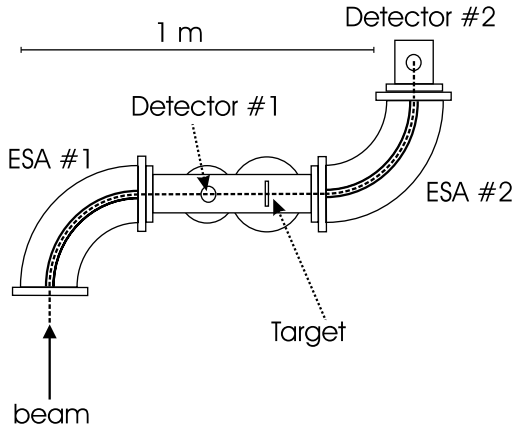

FIG. 1. Schematic diagram of the stopping-power experiment.

from the RFQ is rather large, the first analyzer is used to select an incident beam with a small energy spread around the energy E_1, which is determined by the voltages applied to the electrodes forming the first ESA. In the case of protons which are usually produced with a well-defined energy, only one ESA would be necessary. After traversal of the target foil of thickness Δx, a second analyzer measures the exit energy distribution of the beam, centered around E_2, by varying the voltages on the ESA. The stopping power is then determined as $-dE/dx = (E_1 - E_2)/\Delta x$ at the average energy $(E_1 + E_2)/2$. The detection of the antiproton beam also poses special problems, partly because of the short pulses which prevent single particle detection, and partly because of the annihilations occurring when antiprotons are stopped in matter. The annihilation results in a signal from the detector which varies substantially between different antiprotons. To detect the antiproton pulse we used two-stage channel-plate detectors with optical readout by CCD cameras from a phosphor screen. The beam profiles obtained with the triggered CCD camera can then be stored for subsequent analysis; for details, see [11]. One detector was positioned after the first analyzer, for tuning of the incident beam, and another one after the second analyzer; see Fig. 1. The position resolution of one CCD of about 1 mm yields an energy resolution of $\pm 0.2\%$ at 10 keV due to the dispersion [12]. Although the apparatus was optimized for measurements with antiprotons, it can be used for any charged particle, i.e., also protons. The whole setup was thoroughly calibrated and tested using protons of known energy [11]. The foils used in the experiment are mounted on tungsten or nickel meshes of approximately 85% transmission (no backing foil). The thicknesses of the foils ranging from 20 to 40 nm were measured absolutely for Al, Ni, and Au using Rutherford backscattering and for C by measurements of energy losses with protons [11]. The background pressure was kept below 10^{-7} Torr.

An advantageous procedure to measure stopping powers at different energies with a beam at a fixed primary energy is to accelerate/decelerate the beam upon entrance and exit of the target foil by biasing the foil [11]. This means that the RFQ and beam line can be left unchanged, and this is important in particular for the rather complicated decelerators used to produce the low-energy antiproton beam.

The stopping power measurements are shown in Figs. 2–5 for carbon (two foils), aluminum, nickel (two foils), and gold (two foils). Results of measurements with protons with our apparatus are shown [11], where □, ○, and △ represent the data sets at primary beam energies of 8, 15, and 23 keV, respectively. The proton stopping powers for carbon, aluminum, and gold recommended by [13], and in the case of nickel by [14], are shown as the upper full drawn curves. We notice that our proton measurements agree with these stopping power values over almost 2 orders of magnitude in energy.

Measurements of antiproton stopping powers of the four elements were made in the energy range 5–70 keV, and in addition in the case of carbon down to 1.5 keV. The measurements were made at several primary antiproton energies from the RFQ of 18, 23, 30, 43, and 63 keV as marked with the symbols ◆, ●, ■, ▼, and ▲. The origin of the scatter in the data points is not statistical but is due to fluctuations in the antiproton intensity from pulse to pulse as the average exit energy of the antiprotons is found by combining several beam profiles to get the energy loss distribution. This results in a general uncertainty on the stopping power of $\simeq 15\%$. Within this uncertainty there is a good overall agreement between the different measurement series in the overlap regions. In addition, we see that the new antiproton data merge with the previously obtained data [8], shown using the symbol ★, in the overlap regions for the case of aluminum and gold. This adds confidence to the new measurements, since the previous data were obtained with a completely different experimental technique.

The measurements show a reduced stopping power for antiprotons as compared to protons. The reduction in the investigated energy region below the stopping-power

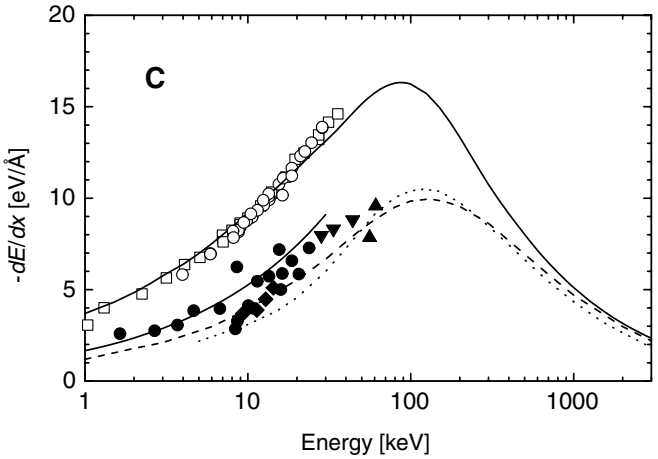

FIG. 2. Measured antiproton (filled symbols) and proton (open symbols) stopping powers of carbon. See the text for explanation of the curves.

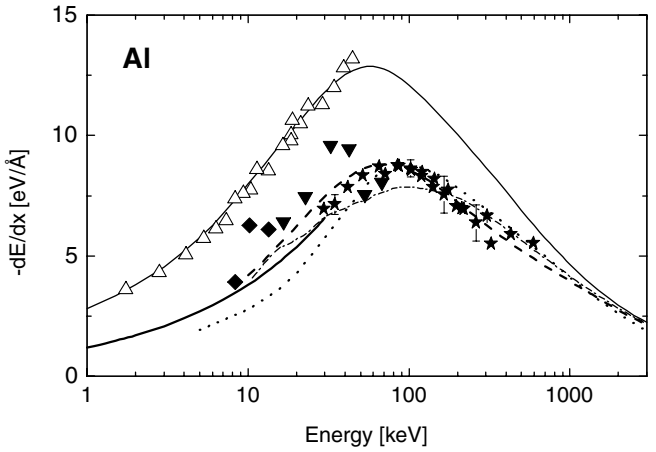

FIG. 3. Measured antiproton (filled symbols) and proton (open symbols) stopping powers of aluminum. See the text for explanation of the curves.

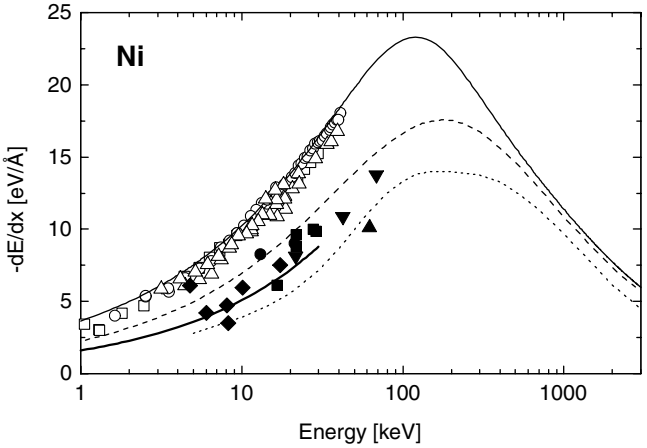

FIG. 4. Measured antiproton (filled symbols) and proton (open symbols) stopping powers of nickel. See the text for explanation of the curves.

maximum is almost a factor of 2 for all the targets but Al. The main experimental result is the linear velocity dependence of the stopping power in the investigated low-energy region. In order to establish the linearity, the data for the four different elements were fitted by $-dE/dx = av^b$, where a and b are free parameters and v is the projectile velocity. Only data below 30 keV, which is significantly below the maximum, were used. The data are shown in Fig. 6 together with the obtained fits. The resulting velocity exponents b are 0.96 ± 0.14, 0.89 ± 0.30, 1.00 ± 0.17, and 0.81 ± 0.14 for carbon, aluminum, nickel, and gold, respectively. This is in good agreement with the predicted exponent of 1 from the free-electron-gas model.

The stopping power data are compared with several theoretical models in Figs. 2–5. One set of models is based on a free-electron-gas description of the stopping medium [2]. Several approaches have been developed, and some also for the rather complicated case of non-negligible target electron velocities. Here we mention the density-functional theory [15] and the calculation using the "extended Friedel sum rule" [16]. The latter model, applicable around and above the stopping power maximum, is shown in the figures as dotted lines. This model seems in general to give slightly too low stopping powers below the maximum. At high energy, this calculation also does not merge with the recommended proton curve for Au and Ni. Sørensen [17] developed a simple approach, which is valid only in the limit of small projectile velocities. This asymptotic stopping power is shown as the lower full drawn curves. We observe that this model agrees very well with the measurements for all target materials apart from aluminum.

Mikkelsen and Sigmund [18] developed a quantum-mechanical harmonic oscillator model within the framework of perturbation theory. Results of calculations including the first three leading terms are shown as dash-dotted curves in Figs. 3 and 5. Although there is in general a qualitative agreement with the measurements, the calculated stopping power around the maximum is clearly too low for aluminum and too high for gold. Furthermore, the velocity dependence at low energy is clearly much too steep for gold. However, as mentioned, this calculation is a perturbation calculation and the convergence of the series expansion can not be assured around and below the stopping power maximum.

Finally, we mention the binary stopping theory by Sigmund and Schinner [19,20]. This theory is a classical binary scattering theory, where the harmonic potential used by Bohr [1] is replaced by an effective screened potential, which in turn is obtained from oscillator strengths derived from tabulated optical properties. The results from this calculation are shown as dashed lines in the figures. This theory successfully reproduces our previous antiproton stopping powers at and above the stopping-power maximum [8,19]. The theory is also able to reproduce most features of the present measurements at much lower

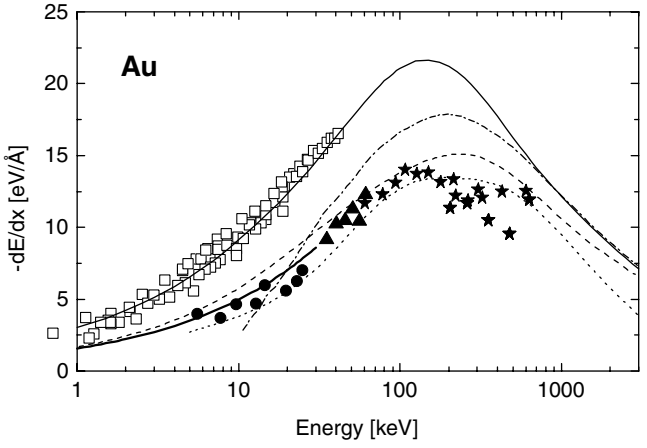

FIG. 5. Measured antiproton (filled symbols) and proton (open symbols) stopping powers of gold. See the text for explanation of the curves.

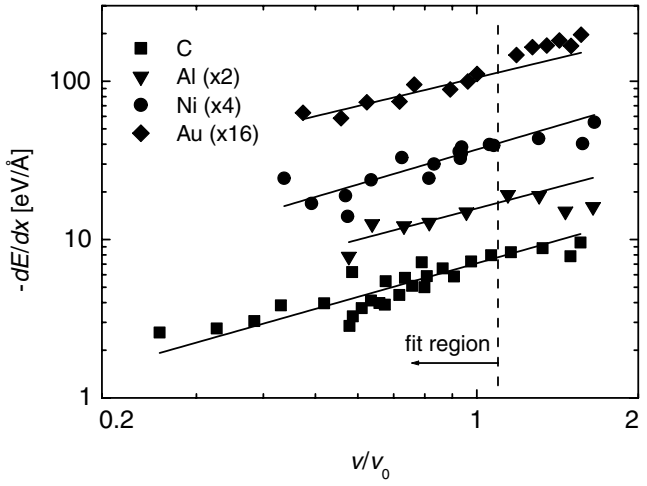

FIG. 6. Measured stopping powers as function of projectile velocity, normalized to the Bohr velocity. The linear fits to the data below the dotted line are also shown. Notice the two logarithmic axes.

energies. Looking in detail at the new results, there are, however, significant deviations of the order of 20%–30%. For example, for Ni and Au, the model results are too high, whereas they seem to be too low for C and Al. This might be explained by the choice of the optical data used as input data in the calculation.

In conclusion, antiproton stopping powers were measured in hitherto unexplored energy regions. Large reductions in the stopping power of antiprotons as compared to protons are observed below the stopping-power maximum. The data obtained with the negative, pointlike projectiles constitute an unequivocal confirmation of the archetype velocity-proportional stopping power at low energy. In addition, the experiment provides reference data for present and future theories.

This work has been supported by the ICE center and a Steno scholarship, both under the Danish Natural Science Research Council (SNF). We acknowledge P. Sigmund, A. H. Sørensen, and A. Svane for providing the calculations of the binary and the free-electron-gas models. We also acknowledge the technical help of CERN staffs and the assistance and advice from collaborators within the ASACUSA Collaboration.

[1] N. Bohr, Philos. Mag. **25**, 10 (1913).
[2] E. Fermi and E. Teller, Phys. Rev. **72**, 399 (1947); J. Lindhard, K. Dan. Vidensk. Selsk. Mat. Fys. Medd. **28**, No. 8 (1954).
[3] M. Famá *et al.,* Phys. Rev. Lett. **85**, 4486 (2000).
[4] R. Golser and D. Semrad, Phys. Rev. Lett. **66**, 1831 (1991).
[5] A. Schiefermüller *et al.,* Phys. Rev. A **48**, 4467 (1993).
[6] K. Eder *et al.,* Phys. Rev. Lett. **79**, 4112 (1997).
[7] W. H. Barkas, W. Birnbaum, and F. M. Smith, Phys. Rev. **101**, 778 (1956).
[8] S. P. Møller, E. Uggerhøj, H. Bluhme, H. Knudsen, U. Mikkelsen, K. Paludan, and E. Morenzoni, Phys. Rev. A **56**, 2930 (1997).
[9] S. Maury, in *Proceedings of the 2001 Particle Accelerator Conference, Chicago, 2001,* edited by P. Lucas and S. Webber (IEEE, Piscataway, NJ, 2001), p. 580.
[10] W. Pirkl, A. M. Lombardi, and Y. Bylinsky, in *Proceedings of the 2001 Particle Accelerator Conference, Chicago, 2001* (Ref. [9]), p. 585.
[11] H. H. Andersen *et al.,* Nucl. Instrum. Methods Phys. Res., Sect. B (to be published).
[12] T. Azuma *et al.,* ASACUSA Progress Report, CERN Report No. CERN/SPSC 2000-04, 2000, p. 18.
[13] ICRU (International Commision for Radiation Units) Report 49, Stopping Powers and Ranges for Protons and Alpha Particles, 0-913394-47-5, 1993.
[14] H. H. Andersen and J. F. Ziegler, *Hydrogen Stopping Powers and Ranges in all Elements* (Pergamon Press, Elmsford, NY, 1977).
[15] I. Nagy *et al.,* Phys. Rev. B **40**, 11 983 (1989).
[16] N. R. Arista and A. F. Lifschitz, Nucl. Instrum. Methods Phys. Res., Sect. B (to be published).
[17] A. H. Sørensen, Nucl. Instrum. Methods Phys. Res., Sect. B **48**, 10 (1990).
[18] H. H. Mikkelsen and P. Sigmund, Phys. Rev. **40**, 101 (1989).
[19] P. Sigmund and A. Schinner, Eur. Phys. J. D **15**, 165 (2001).
[20] P. Sigmund and A. Schinner, Nucl. Instrum. Methods Phys. Res., Sect. B (to be published).